Journal of Thermal Analysis and Calorimetry, Vol. 76 (2004) 903–911

THERMAL BEHAVIOUR AND CHARACTERIZATION OF AN IRON ALUMINUM ARSENATE MINERAL Mansfieldite-scorodite series

J. Ma. Rincón[1*], *M. Romero*[1], *A. Hidalgo*[1] *and Ma. J. Liso*[2]

[1]The Glass-Ceramics Group/ Lab. Inst. E. Torroja de CC. Construcción, CSIC, Madrid, Spain
[2]Departement of Crystallography and Mineralogy, University of Extremadura, Badajoz, Spain

(Received September 24, 2003; in revised form March 18, 2004)

Abstract

It has been determined the thermal behaviour at high temperatures of an iron aluminum arsenate mineral first described in the location of La Serena Valley, Extremadura, Spain, which expands until 1173 K contracting later and softening at 1653 K and full melting at 1773 K. The DTA/TG experiment only detects some rearrangement with an endothermic at 1173 K due to the mica mixing. The mineral is a scorodite variety mixed with micaceous clay which has been found as aggregates of pyramidal crystals associated with quartz, wolframite, molibdenite, cassiterite and other secondary minerals in the pegmatite of the San Nicolas mine. The chemical composition, the physico-chemical characteristics such as density and hardness, as well as the thermal behaviour has allowed to conclude that this mineral can be an Al-enriched scorodite (mansfieldite): (Fe, Al) $AsO_4 \cdot 2H_2O$ mixed with illite from the scorodite-mansfieldite series.

Keywords: aluminum iron arsenate mineral, high temperature transformations, illite, mansfieldite, scorodite

Introduction

The arsenic usually occurs as natural and/or combined as arsenium-pyrite or often as different types of arsenates. Both the arsenate and the phosphate mineral classses are described in different mineralogies [1, 2], as a specific and similar group of minerals. The hydrated arsenate minerals contain 2–12 water molecules or even less water molecules. The more simple are the iron containing like, for instance, the scorodite ($Fe^{3+}AsO_4 \cdot 2H_2O$) which crystallizes in the orthorhombic symmetry [3] or the cobalt or nickel ones [4], whose are several also described by Ramdohr [5]. Double arsenates of calcium and magnesium are also described as the picropharmacolite $Ca_4Mg(AsO_3OH)_2(AsO_4)_2 \cdot 11H_2O$ [1] with triclinic symmetry; the tyrolite ($Ca_2Cu_9(OH)_{10}(AsO_4)_4 \cdot 10H_2O$) crystallizing in the probably orthorhombic system;

* Author for correspondence: E-mail: jrincon@ietcc.csic.es

1388–6150/2004/ $ 20.00

Akadémiai Kiadó, Budapest
Kluwer Academic Publishers, Dordrecht

the chalcophyllite with $Cu_{18}Al_2$ $(AsO_4)_4$ $(SO_4)_3$ $(OH)_{24}\cdot 36H_2O$ and tabular crystals with rhomboedric appearance or the pharmacosiderite, an iron and potassium basic arsenate with $KFe_4^{3+}(OH)_4(AsO_4)_3\cdot 6–7H_2O$ formula [2, 6]. These structures are amenable to a number of chemical substitutions; in fact, it is very common that Fe-enriched minerals incorporate Al into their structure [7]. The paragenesis of these minerals use to be related to the pH of the parent solution [8]. Therefore, different types of arsenate and mainly basic arsenates can be found in the nature [9].

The arsenic mineral here investigated is of scientific interest for being described first time in this location in the San Nicolás Mine, Extremadura, the west region of Spain in the Iberian Peninsula, as well as for its application as source of arsenic oxide which is a refining agent for releasing of bubbles in the manufacture of glasses, as insecticide and some other applications for metallic alloying and as active principle for cytostatic of some types of leukaemia. Therefore, the aim of this research has been to characterize this mineral at high temperatures, because of the valuable of the thermal behaviour for characterization of minerals [10–12].

Experimental

Materials

The mineral here characterized was found in the nowadays abandoned San Nicolás mine located approximately at 7 km, SW of the Serena Valley in Badajoz province, Extremadura, Spain [13]. There is in this mine an area of pegmatites associated with quartz veins, N direction 60° E. These pegmatites are under a metamorphic series of armorican quartzites and slates close to an intrusive granitic batolite, whose erosion surface has discovered the apical area of the batolite and the upper contact with the metamorphic series. The slate area is crossed by several veins almost vertical and independent between them, viz: hydrothermal and pegmatitic quartzs. There are gneiss and granite sediments under quartzites and slates [14].

The mineral is known from only one hand specimen in the mining area of 'San Nicolás' which has been an exploitation as wolfram and bismuth [15–17] and is located into irregular cavities of quartz veins over milky quartz surrounded by tungstite ($WO_3\cdot H_2O$) in segmentation and/or in veins. It appears on small quantities, crystallized and forming crystalline aggregates of 4–5 crystals of 3 to 5 mm size, fan shaped, joined at the base and separated at the top showing aggregates with stepped growth and ended on pyramids. The mentioned mineral was found into quartz cavities as an alteration product of the iron minerals mainly arsenopyrite. The mineralization is quartz, illite, feldspars close to this mineral, tungstite, fluorite and molybdenite. The main paragenesis of the deposit is: quartz, wolframite, molybdenite and cassiterite, as well as the secondary minerals: tungstite, arsenopyrite, pyrite, galena, bismutinite, topaz, scheelite, tourmaline, bismite, wulfenite, hematite, siderite, malachite and azurite.

Methods

The X-ray diffraction analysis was collected on a Siemens powder diffractometer (Model D-500) by using the powder method. The microstructure was examined by scanning electron microscopy (SEM) and observations have been carried out by previously cleaning of the mineral surface into an ultrasonic bath with the aim of removing the small particles adhered to the surface of crystals and subsequent coating with a gold sputtered thin layer (approximately 20 nm). A SEM DSM Zeiss-950 equipment working at 30 kV accelerating voltage has been used. The investigated mineral was chemically analyzed using an energy dispersive X-ray (EDX) analysis performed directly over the crystals without gold coating in different areas of the mineral in the same SEM equipment and equipped with a Kevex spectrometer of Si(Li) solid-state and Be window. The EDX spectra were acquired for more than 10 min with dead time less than 10%.

The thermal methods used were: differential thermal (DTA) and thermogravimetric analysis (TG) carried out in a Mettler Thermobalance to 1273 K (1000°C) from powdered sample of the mineral and Heating Microscopy observations until 1773 K (1500°C) by using a Leitz Hot Stage Microscope (HSM) from the powdered and pressed specimen after grinding. The sample observed by HSM was a small cylinder 4 mm height×2 mm diameter obtained from the powdered sample.

Results and discussion

Thermal behaviour on heating in ambient atmosphere

The Fig. 1a–f shows the profile of powdered and pressed sample at different temperatures of heating in a HSM microscope at a heating rate of 10°C min^{-1} and following three runs. It is clear the sample blow up during water loss, not only surface water but mainly crystal water. The mineral expands during heating until 1173 K (900°C) due to decomposition of arsenate structure and micaceous mineral content, contracting at higher temperatures when this is increased from 1473 K (1200°C) . After this at approximately 1653 K (1380°C) the specimen soften and at 1773 K (1500°C) takes the hemispherical shape. The Fig. 2 shows the contraction behavior deduced from the HSM experiment.

After DTA/TG controlled heating it can be seen (Fig. 3) that exists a small endothermic peak at 373 K (100°C) due to the adsorbed surface water followed by a wide endothermic peak showing a lower valley at 1173 K (900°C) where it was observed the expansion of specimen by the heating microscopy. In fact, DTA shows three different processes: 1) Endothermic corresponding to water losses in the 353–373 K (80–100°C) due to the adsorbed water in the surface of mineral; 2) a small wide exothermic band at 613 K (340°C) due probably to a release of strain in the lattice of the dioctahedral micas present in the mineral and 3) a broad endothermic band from 673 to 1173 K (400- 900°C) due to losses of constitutional water and final volatilization of free arsenic cations. In the same zone occurs the

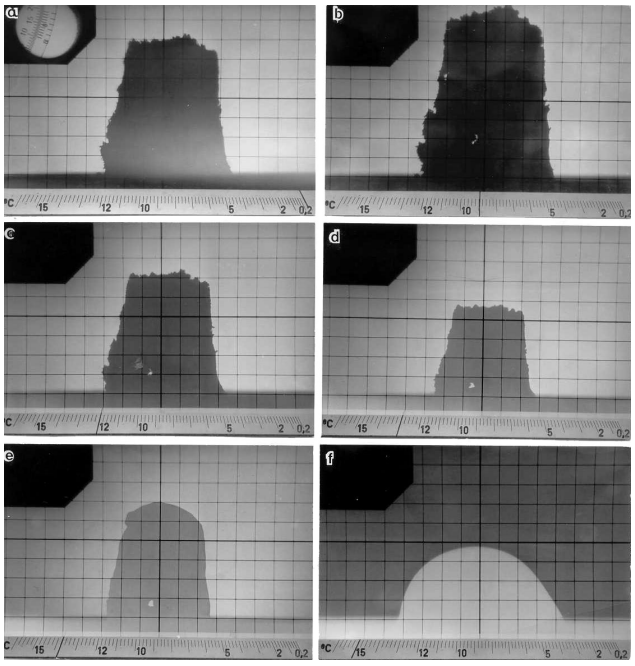

Fig. 1 HSM observations of thermal behaviour until 1500°C of Al-scorodite found in Extremadura, Spain: a – at ambient temperature; b – some expansion can be seen at 900°C; c – starting contraction at 1200°C; d – progressing increase of contraction at 1300°C; e – softening point at 1380°C and f – hemispherical shape formation at 1500°C

dehydroxylation of illite which can loss its structure water between 823 and 993 K (550–720°C) [18] starting at 1173 K the sintering detected by HSM from the residual iron and aluminum oxide species. The observed endothermic between 1123 and 1223 K (850–950°C) is composed by two peaks: The first one can be assigned to the dehydroxylation of the dioctahedral micas with subsequent rearrangement and the

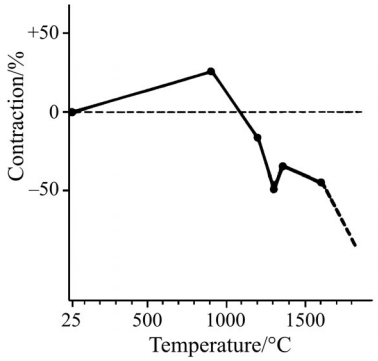

Fig. 2 Contraction behavior deduced from the HSM micrographs

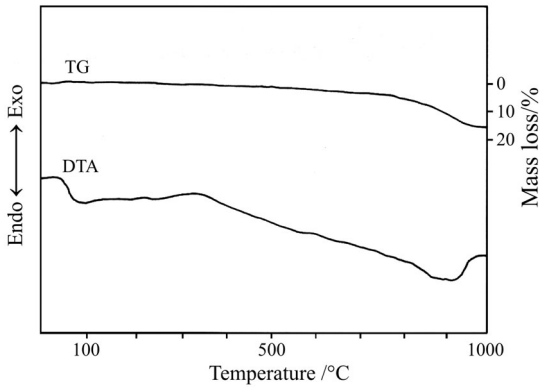

Fig. 3 DTA/TG traces of the Al-scorodite found in Extremadure, Spain. The DTA shows three different processes: 1 – endothermic corresponding to water losses in the 80–100°C; 2 – small exothermic at 340°C due to transformation of arsenic ions and 3 – endothermic at 900°C due to volatilization of arsenic cations

second one might be assigned to the maximum contraction after volatilization of As, and the non-volatile elements which might form the binary compound: $Fe_2O_3 \cdot Al_2O_3$ from an iron spinel which is oxidized on heating. This can be in agreement to the exothermic trend observed at 1273 K (1000°C). The presence of illite impurities in this mineral series can give rise at higher temperatures to the formation of a glassy product which melts at 1773 K (1500°C). On the other hand, the TG curve depicts a continuous loss from room temperature, when is starting the decomposition of the mineral and an increase of the slope between 973–1173 K (700–900°C), corresponding to the endothermic peaks above discussed.

Physical properties and microstructure

The mineral here described is light grey–greenish in colour, transparent, strong vitreous bright with white streak. Studied under transmitted light this mineral shows refraction index of: $\omega = 1.667$ and $\varepsilon = 1.642$ ($\omega = R_0$ and $\beta = R_{extra}$) and it is not pleochroic. (Stoichoimetric scorodite is biaxial, orthorhombic, with refraction indexes of $\alpha = 1.784$, $\beta = 1.795$ and $\gamma = 1.814$). It has a hardness of approximately 2 in the Mohs scale and density measured with heavy-liquid techniques in 2.95 g cm^{-3}. Both are low in comparison with conventional scorodite might be caused by impurities (illite, quartz) as well as by inclusions (air bubbles at the boundary of crystal fragments and/or presence of hydrogen and/or hydroxyls, such as is usual in other arsenate minerals) [8].

The Fig. 4a has been taken with back-scattered electrons (BSE) showing additional contrast due to the atomic number differences in the mineral and the Figs 4b and 4c correspond to secondary electron images. The observed crystals are prismatic and aggregated along the longer dimension being 50–200 μm in length and average width ranged between 10–100 μm. As was previously explained, they form

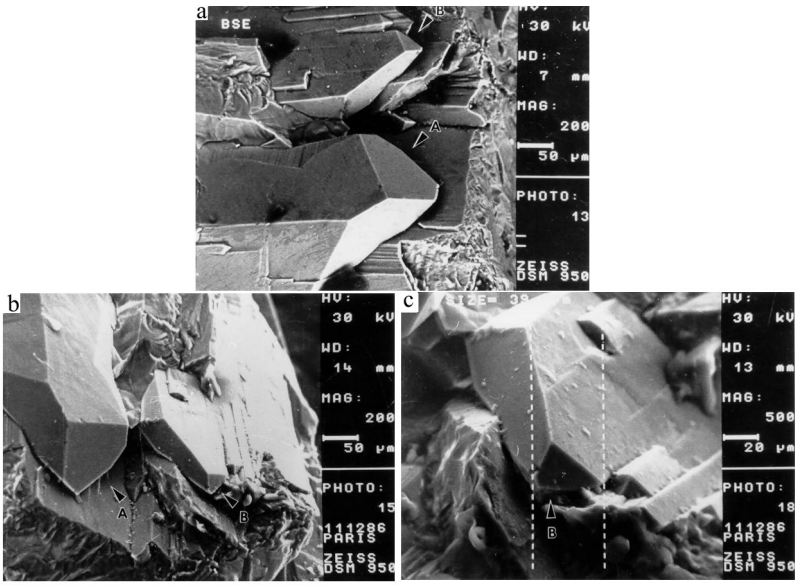

Fig. 4 SEM micrographs obtained from Al-scorodite showing different contrast due to back-scattered and secondary electron image at x 200 magnification a – and b – and c – at x 500 magnification, respectively (the parallel lines in c) micrograph indicate the width of a plane perpendicular to the rhomboedric crystals and analyzed area by EDX) (the A and B labels in the pictures indicate the same truncated faces which are rotated 90° angle in the b) micrograph with respect the a) picture. The same B face appears at higher magnification in the micrograph c))

crystalline aggregates of 4–5 crystals of 3 to 5 mm size, fan shaped, joined at the base and separated at the top showing aggregates ended on rhomboedres and pyramids. In the case of these aggregates were twinned, the twin laws were not determined in this case, because only SEM observations were carried out in this case and these crystallographic relations only could be determined by electron diffraction through out TEM observations

Chemistry and crystallographic characterization

From the EDX spectra the K_α and K_β X-ray emissions of Fe were clearly identified (6.40 and 7.06 keV respectively) and the L_α X-ray emission of the same element (0.70 keV). Moreover, the K_α and K_β emissions of As can be identified (10. 53 and 11. 73 keV respectively) as well as the L_α As band (1.28 keV) which is overlapped with the K_α X-ray emission of magnesium (1.25 keV). Therefore, as the mineral here described contains As, this overlapping do not allow us to elucidate if magnesium is an element included in this mineral. Likewise, the K_α X-ray emission of Al (1.49 keV) was clearly identified in the expanded spectrum as well as a small

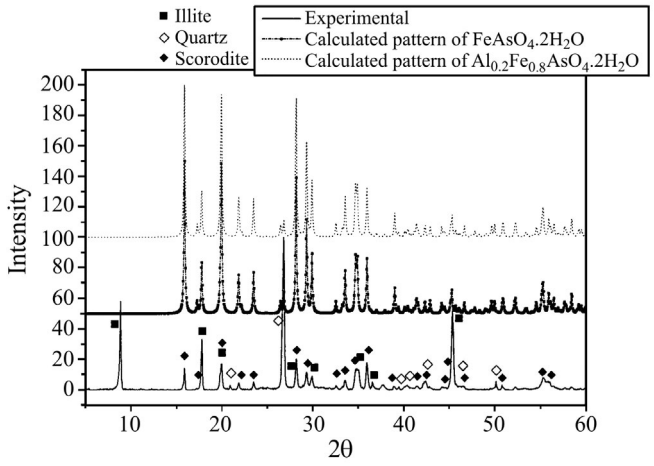

Fig. 5 Experimentally observed X-ray powder diffraction pattern of the mineral, and calculated patterns of $FeAsO_4{\cdot}2H_2O$ (scorodite) and approximate formula: $Al_{0.2}Fe_{0.8}\ AsO_4{\cdot}2H_2O$

quantity of Si due to the presence of the K_α band (1.74 keV) overlapped with the Al emission. In addition to the formed bands a little K_α X-ray emission band of the potassium (3.30 keV) has been identified.

In other areas focusing the electron beam in spot mode on crystals of this mineral is found also As, Al and Fe, without detecting Si and K as in the average spectra. Therefore, this mineral found in San Nicolás Mine, Spain, contains basically: As, Fe, Al and as minor components of Si and K, though due to the low analytical space resolution of the SEM/EDX system can be due to clayish minerals associated and close to this mineral. The quantitative analysis, performed with the Kevex software based on the Colby method [19] by using as standards: InAs for arsenic (L_α emission), metallic iron for iron (K_α emission) and Al_2O_3 for aluminium (K_α emission), gives the following average composition: 57.18% As_2O_5, 25.08% Fe_2O_3 and 17.74% Al_2O_3, which shows an excess of aluminium oxide with respect the mansfieldite and intermediate compounds in the scorodite–mansfieldite series [9]. This fact can be due to the presence and/or mixing of micaceous clay (illite) embedding the surface of the mineral crystals.

The X-ray powder diffraction pattern of the mineral is given in Fig. 5. Three different mineral phases were identified in the sample: illite, quartz (SiO_2) and Al-scorodite (Fe, Al)$[AsO_4]{\cdot}H_2O$, being illite the major secondary crystalline constituent. Though the presence of these secondary phases complicate the crystallographic analysis, by looking at calculated patterns, it can be noticed that those vary slightly when a 20% of Al is substituted by Fe. Then, unit cell parameters of Al-scorodite were determined using the program TREOR90 [20]. Calculations involved the fitting of the experimental peaks identified as scorodite, with calculated profiles and background. The *c* parameter agrees well within 0.010 Å with values

reported by Hawthorne for scorodite [8]. However, parameters *a* and *b* are shorter than the reported values, 0.009 Å shorter in the *a* direction and 0.002 Å shorter in the *b* direction. The range of such differences are not surprise for secondary minerals. In the simplest case, the substitution of aluminium by iron also detected by the EDX microanalysis is expected to contract the crystalline lattice, since the ionic radii of Al is shorter than the radius of Fe. Then, according to this result, a partial substitution of Al by Fe would be possible in the mineral, matching well the XRD diagramme of the formula: $Fe_{0.80}Al_{0.20}AsO_4$, closed to the SEM/EDX microanalytical results and after considering the water content (16%) calculated from the TG analysis. Therefore, this mineral is a member of the scorodite ($FeAsO_4 \cdot 2H_2O$) – mansfieldite ($AlAsO_4 \cdot 2H_2O$) series of minerals [9].

Conclusions

Research carried out by TG and DTA, as well as HSM has allowed the full characterization and follow of thermal decomposition at high temperatures of an arsenate mineral described first time in the San Nicolas mine of Extremadura, Spain. It was deduced that this mineral is an aluminium scorodite in the scorodite–mansfieldite series being associated with illite which decomposes as:

$$2\ AsO_4(Al, Fe)\cdot 2H_2O \rightarrow Al_2Fe_2O_4 + As_2O_3 \uparrow + 2H_2O \uparrow + 1/2O_2 \uparrow$$

The mineral here described is intermediate in the mentioned mansfieldite–scorodite series due to the presence of high aluminium oxide content and intermediate values in the physical properties such as refraction index and specific volume from the pure scorodite. The mineral is also similar to some mansfieldite, where substitutions of aluminium by iron are higher than described before.

* * *

Many thanks are due to J. M. Bassas, University of Barcelona, for carrying out the XRD experiments, as well as to A. Pérez Garrido from the University of Extremadura, Spain.

References

1 A. R. Hölzeln, Systematics of Minerals, Ober-Olm Germany, 1999.
2 C. Palache, H. Berman, C. D. Frondel, D. Dana and J. E. Salisbury, System of Mineralogy, John Wiley and Sons Inc., New York 1963, Vol. II, 7th Edition, p. 765.
3 P. Ondrus, R. Skála, C. Viti, F. Veselovsky, F. Novák and J. Jansa, Am. Mineral., 84 (1999) 1439.
4 A. C. Roberts, P. C. Burns, R. A. Gault, A. J. Cridle, M. Feinglos and A. R. Stirling, Eur. J. Mineral., 13 (2001) 167.
5 P. Ramdohr, Klockmann Lehrbuch der Mineralogie. 14 Ed. Ferd. Enke Verlag. Stuttgart 1954.
6 R. J. Davis and M. H. Hey, Mineralogical Magazine, 33 (1964) 937.
7 F. D' Ivoire and M. Rowis, Comptes Rendus, 267 C (1968) 955.
8 F. C. Hawthorne, Acta Crystallogr. B, 32 (1976) 2891.
9 V.T. Allen and J. J. Fahey, American Mineralogist, 33 (1948) 122.

10 A. Acosta, I. Iglesias, M. Aineto, M. Romero and J. Ma. Rincón, J. Therm. Anal. Cal., 67 (2002) 249.
11 H. Zou, M. Li, J. Shen and A. Auroux, J. Therm. Anal. Cal., 72 (2003) 209.
12 A. Fodor, L. Ghizdavu, A. Suteu and A. Caraban, J. Therm. Anal. Cal., 75 (2004) 153.
13 P. Florido, M. Alvarado and P. García, La Minería en Extremadura, ENADIMSA and Junta de Extremadura, Eds, D^{on}. General de Industria, Energía y Minas, Madrid, 1977, p. 81.
14 J. García Guinea, Ma. J. Liso and E. Galan, Estudios Geológicos, 34 (1978) 139.
15 P. Gumiel, Chronique de la Recherche Minière, 463 (1981) 5.
16 P. Gumiel and A. Pineda, Tecniterrae, 39 (1981) 16.
17 F. Tornos and P. Gumiel, El wolframio y estaño: Aspectos económicos y metalogénicos, in: Recursos Minerales de España, J. García Guinea and J. Martínez Frías, Editors) CSIC, Madrid 1992.
18 T. Hatakeyama and Zhenhai Liu, Handbbok on Thermal Analysis, John Wiley and Sons, New York 1998.
19 R. Woldseth, Quantitative Analysis, In: X- ray Spectroscopy, Kevex Corp, Burlingame, California 1973, p 18.
20 E. Werner, L. Erikson and M. Wesdahl, J. App. Crystallogr., 18 (1985) 367.